Emergent Orientation Maps —— Mechanisms, Coding Efficiency and Robustness

Haixin Zhong (presenter), Haoyu Wang, Wei P Dai, Yuchao Huang, Mingyi Huang, Rubin Wang, Anna Wang Roe, *Yuguo Yu

hxzhong@fudan.edu.cn & *yuyuguo@fudan.edu.cn

------- *International Conference on Learning Representations (2025)* -------

Spatial arrangements of V1 organizations

- Two primary visual cortex (V1) spatial arrangements have been discovered: **pinwheel structures** (Higher mammals) and **salt-and-pepper organizations** (Lower mammals).
- Classical self-organizing feature maps explain orientation maps via **local cooperation** and **winner-take-all** dynamics *(Kohonen, 1982, Biol. Cybern.)*.
- Recent studies highlight the role of multiscale biological factors – such as **synaptic plasticity**, **visual input overlap**, and **wiring constraints** in shaping pinwheels. *(Chalk et al., 2018, PNAS; Boutin et al., 2022, PLOS Comput. Biol.; Najafian et al., 2022, Nat. Comms.; Jang et al., 2020, Cell Rep.; Koulakov & Chklovskii, 2001, Neuron)*

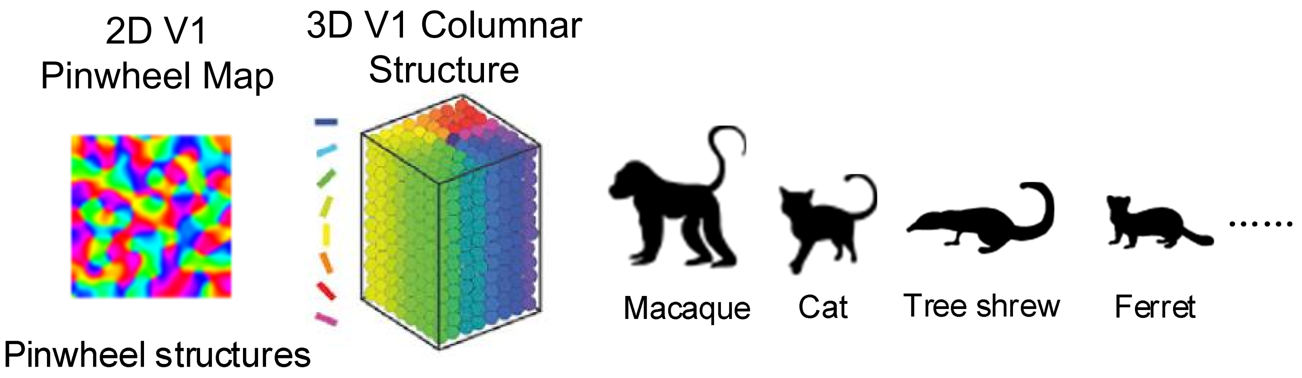

(Ho et al., 2023, Curr. Biol.)

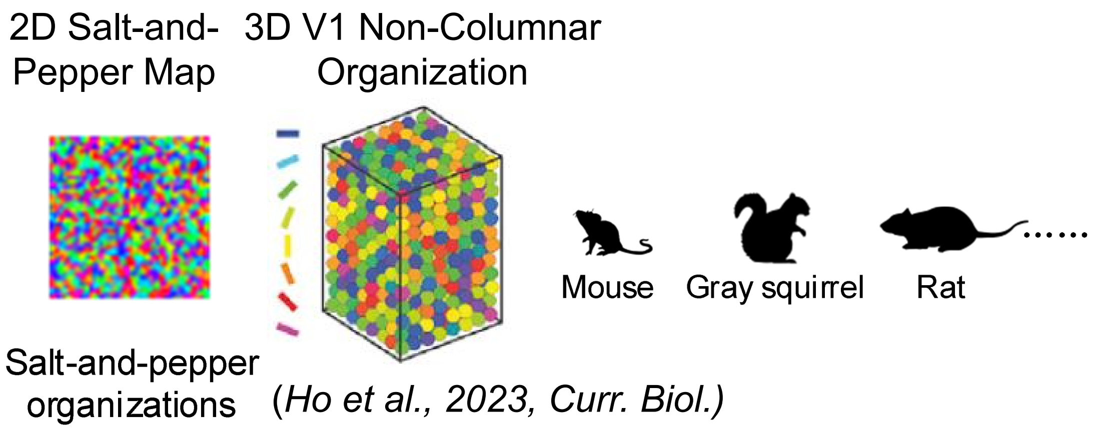

(Ho et al., 2023, Curr. Biol.)

Spatial arrangements of V1 organizations

- However, these studies typically examine these factors in isolation, and **the coordinated mechanisms by which they shape and refine orientation topologies during development remain unclear**.

What neural plasticity dynamics govern the coordinated emergence and refinement of orientation maps, and how do these structures contribute to the computational efficiency and robustness of visual coding?

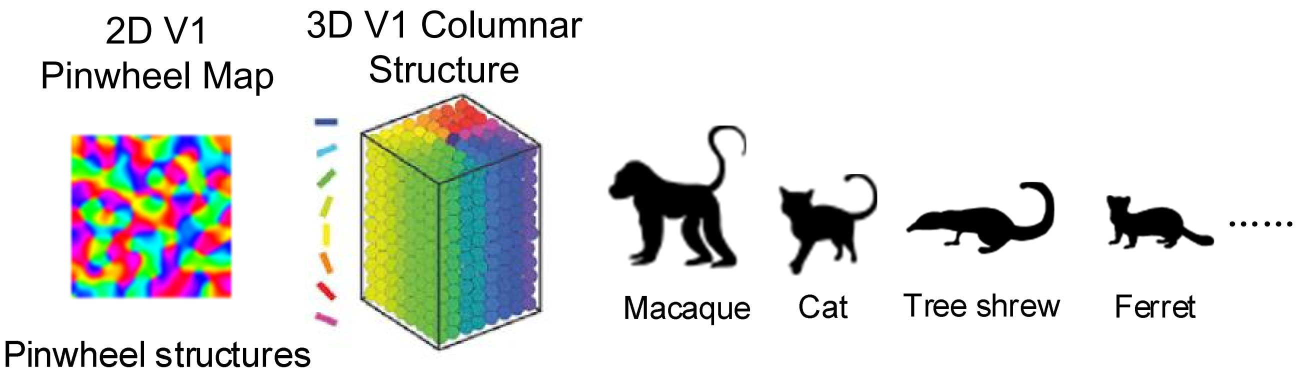

(*Ho et al., 2023, Curr. Biol.)*

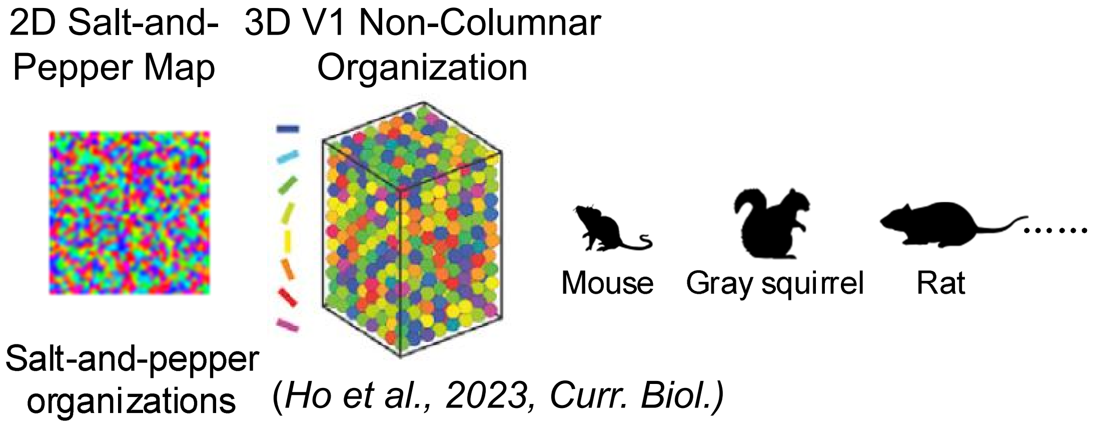

(*Ho et al., 2023, Curr. Biol.)*

Anatomical data suggests RFs density underlying V1 organizations

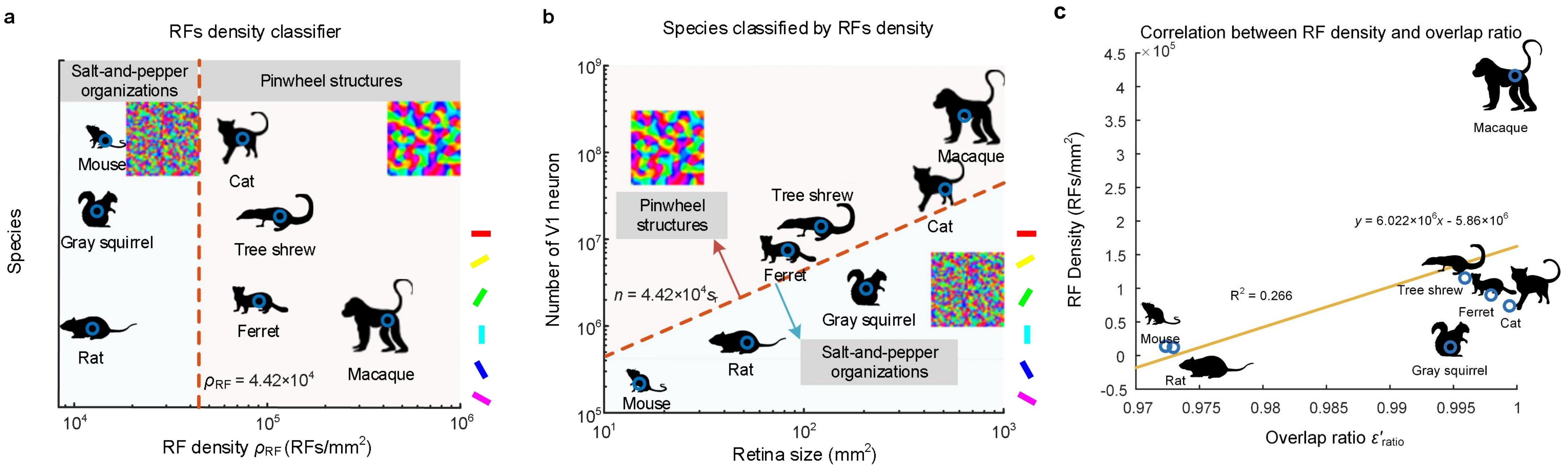

V1 receptive field density serves as the linear classifier (Data: Retina size, V1 size, V1 neurons density, RF size):

1. We conduct a statistical analysis of anatomical data from seven species and find that the receptive field density ρ_{RF} in V1 can act as a linear classifier to distinguish species with "pinwheel" or "salt-and-pepper" structures. (Figs. a and b)

2. In these anatomical data, the factor influencing receptive field density is the visual field overlap (ε ').

(Srinivasan et al., 2015, *Nature Neuroscience*), (Tehovnik et al., 2007, *Journal of Neurophysiology*), (Scholl et al., 2013, *Neuron*), (Veit et al., 2014, *Journal of Neurophysiology*), (Engelmann et al., 1996, *Journal of Comparative Neurology*), (Weigand et al., 2017, *Vision Research*), (Law et al., 1988, *Brain Research*), (Huberman et al. ,2006, *Nature*), (Niell et al., 2008, *Neuron*), (Van Beest et al. ,2021, *Cell Reports*), (Foik et al., 2020, *eLife*)。

Self-evolving spiking neural network

Retinotopic maps of functional activity

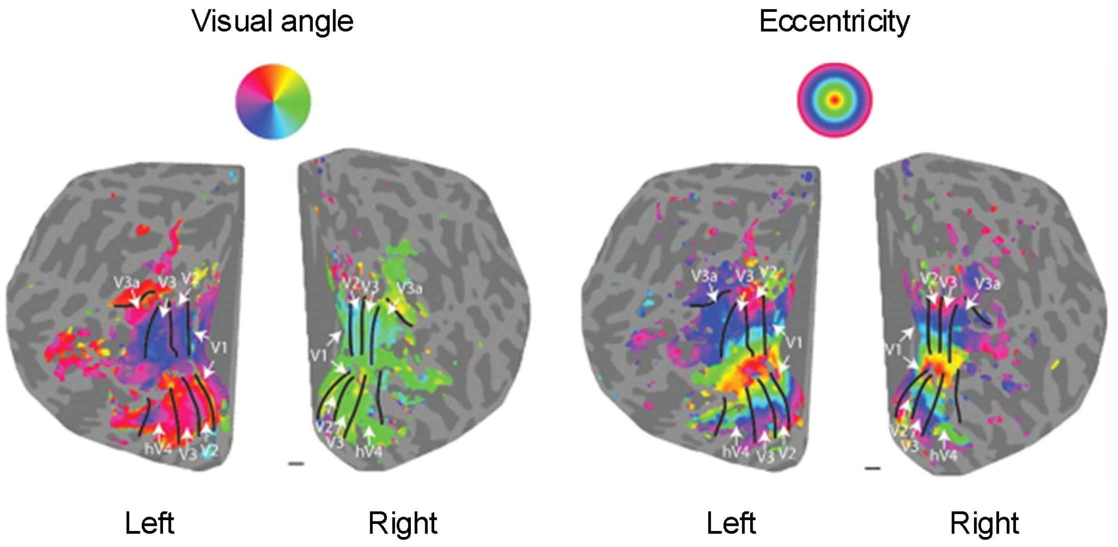

(Holly Bridge et al., 2013, J. Neurosci.)

Self-evolving spiking neural network (SESNN)

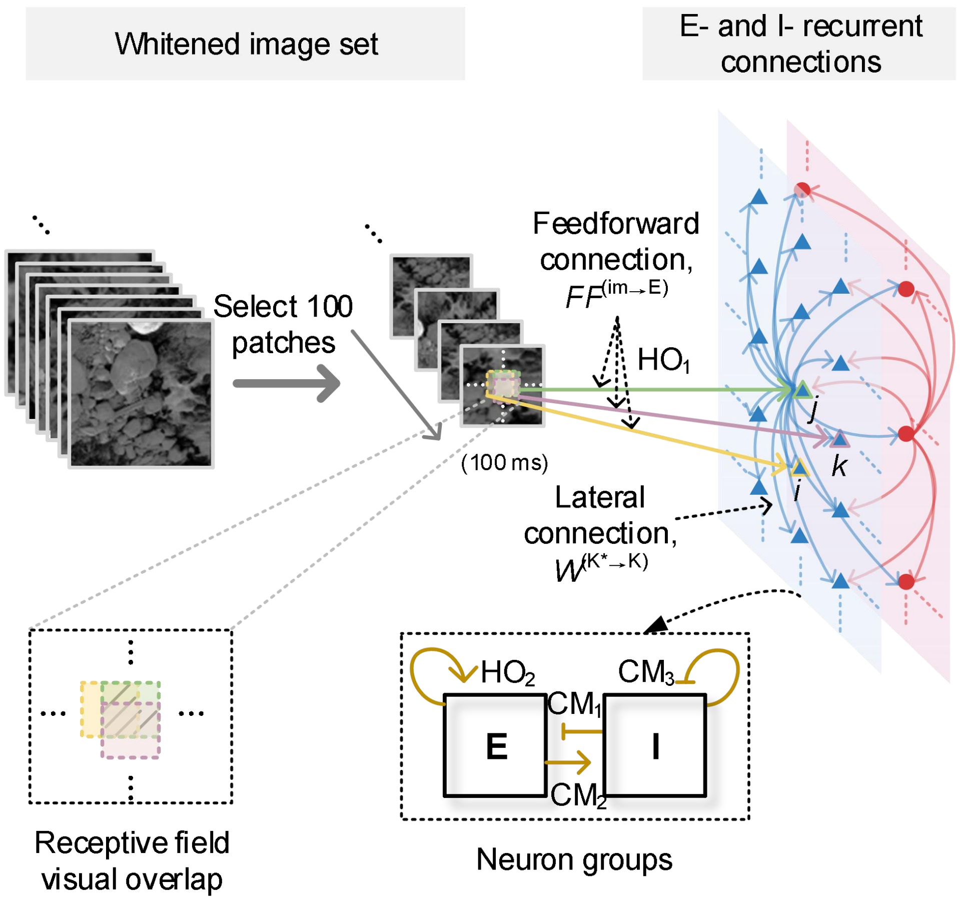

E-neuron — E-connection
I-neuron — I-connection

Unlike ANN and rate-based models that ignore anatomical factors, our SESNN computational model incorporates comprehensive data, including retinal topology, neuronal morphology, and neural connectivity. The network evolves based on neural plasticity.

Self-evolving spiking neural network

SESNN model

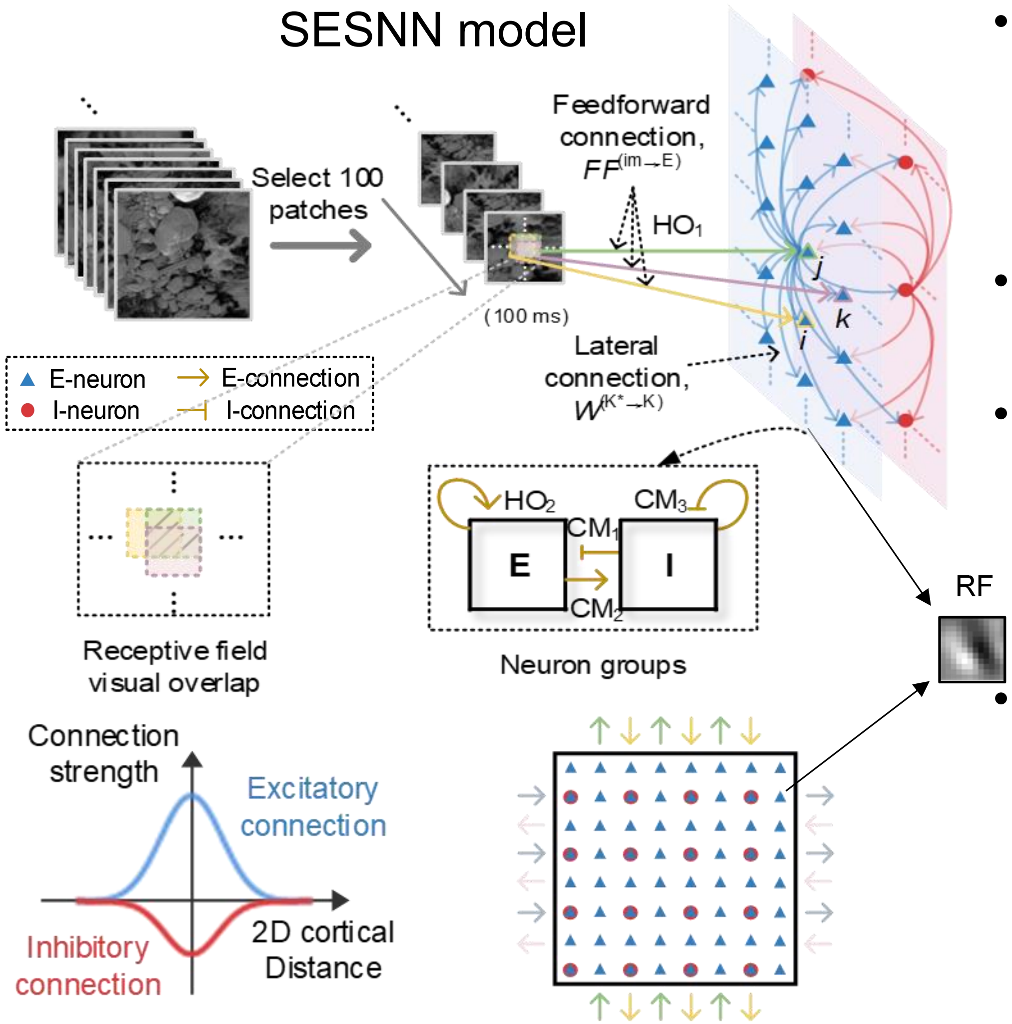

- **Select Patches**: Randomly select 100 patches, each of which is presented to all E-neurons for 100 *ms* (100 time steps).
- **Overlap**: Neighboring neurons share overlapped inputs.
- **Neural connectivity**: $W_0{}^{K'\to K}(i,j) = \alpha_{K'} \times \exp(\frac{-d(i,j)^2}{2\sigma_{K'}^2})$.

  $d(i,\ j)$: Euclidean distance from neuron i to neuron j.

  $\alpha_{K'}$: maximum connection weight.
- **Neuron model**: E- and I- leaky integrate-and-fire neurons.

$$u_i^{(K)}(t+1) = u_i^{(K)}(t)e^{-\frac{1}{\tau^{(K)}}} + h_E(i)\sum_m FF_{im}^{(image\to E)} X_m + \sum_{K^*}\sum_i \beta_{ij}^{(K^*\to K)} \cdot W_{ij}^{(K^*\to K)} \cdot z_j^{(K^*)}(t) + noise$$

$$h_K(i) = \begin{cases} 1 & \text{if } i \text{ is an E-neuron ID} \\ 0 & \text{if } i \text{ is an I-neuron ID} \end{cases},$$

Zhong et al. Emergent Orientation Maps —— Mechanisms, Coding Efficiency and Robustness. *ICLR 2025 spotlight.*

Self-evolving spiking neural network

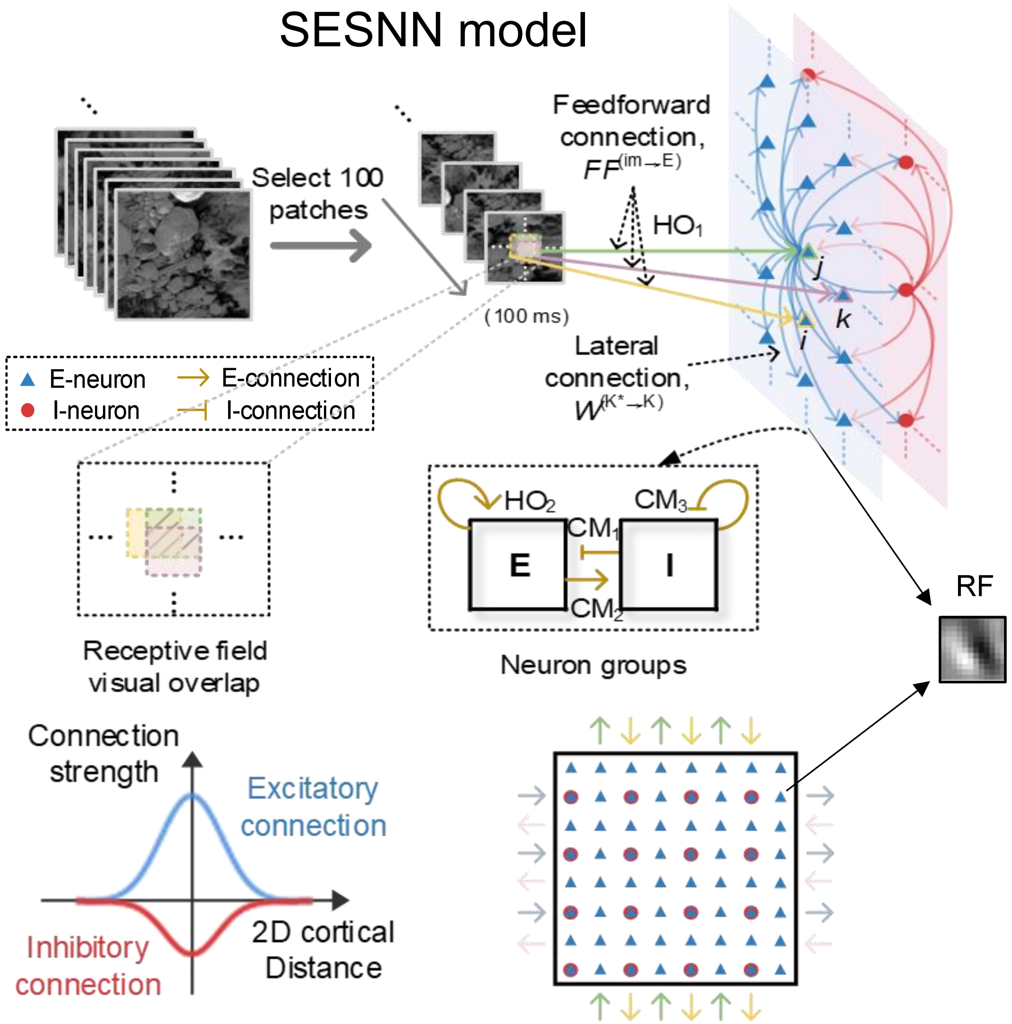

- **Hebbian-Oja (HO) (FF and EE):**

$$\Delta FF_{im}^{(\mathrm{Img}\to\mathrm{E})} \propto y_i x_m - y_i^2 FF_{im}^{(\mathrm{Img}\to\mathrm{E})}, \quad \langle y_i x_m\rangle - \langle y_i^2\rangle FF_{im}^{(\mathrm{Img}\to\mathrm{E})} = 0$$

$$FF_{im}^{(\mathrm{Img}\to\mathrm{E})} = \frac{\langle y_i x_m\rangle}{\langle y_i^2\rangle} = \frac{STA_i}{\langle y_i^2\rangle} \xrightarrow{\text{FF}}$$ Learn receptive field

$$\Delta W_{ij} \propto y_i x_j - y_i^2 W_{ij} \xrightarrow{\text{EE}}$$ Prevent over-excitation

- **Correlation Measuring (CM) (Other types of connections):**

CM rule ensures orientation diversity and map coverage via E-I-E loops.

$$\text{CM: } \Delta W_{ij} \propto y_i x_j - \langle y_i\rangle\langle x_j\rangle(1 + W_{ij})$$

$$W_{ij}^{(\mathrm{K}^*\to\mathrm{K})} = \frac{\langle y_i x_j\rangle - \langle y_i\rangle\langle x_j\rangle}{\langle y_i\rangle\langle x_j\rangle} = \frac{\mathrm{Cov}(y_i, x_j)}{\langle y_i\rangle\langle x_j\rangle} = \frac{\mathrm{Cov}(y_j, x_i)}{\langle y_j\rangle\langle x_i\rangle} = W_{ji}^{(\mathrm{K}^*\to\mathrm{K})}$$

Predictive coding through E-I-E loops, remove coding redundancy, sparse coding

Zhong et al. Emergent Orientation Maps —— Mechanisms, Coding Efficiency and Robustness. *ICLR 2025 spotlight.*

Role of visual field overlap in determining V1 organizations

- The level of visual field overlap between neighboring neurons in V1 determines the formation of distinct orientation maps:
  Formation of pinwheel structures at high overlap.
  Formation of salt-and-peppers at lower overlap.

Role of overlap

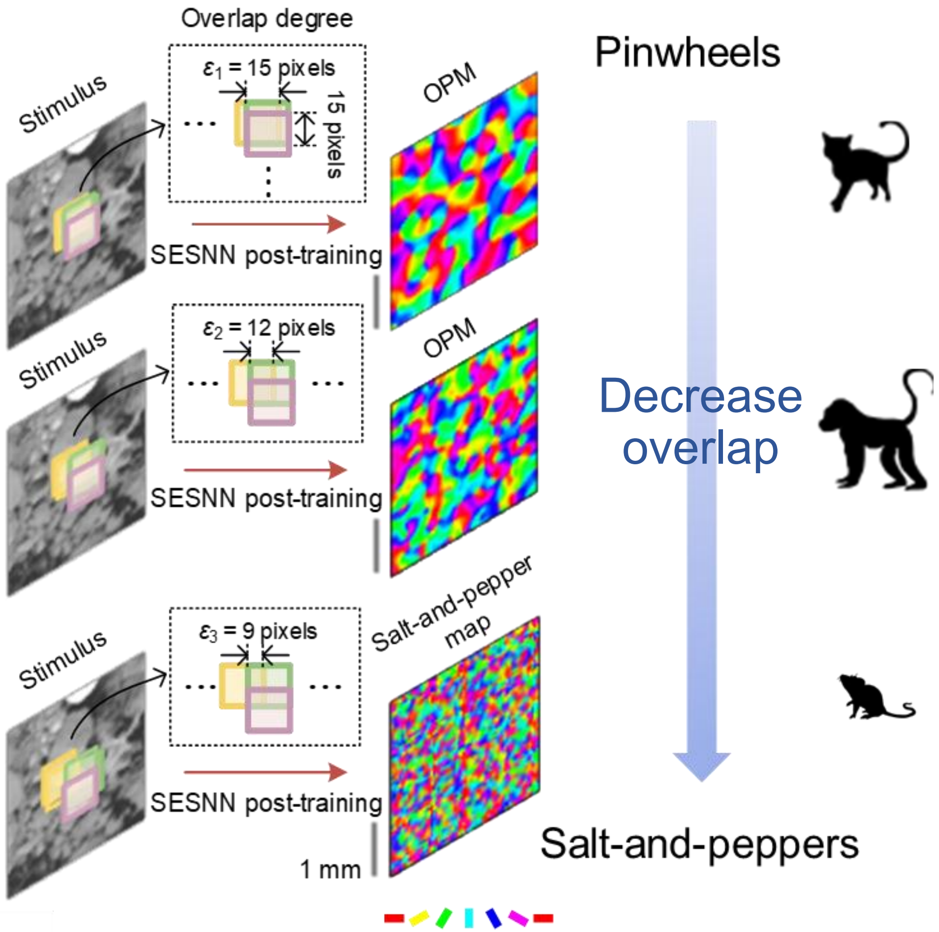

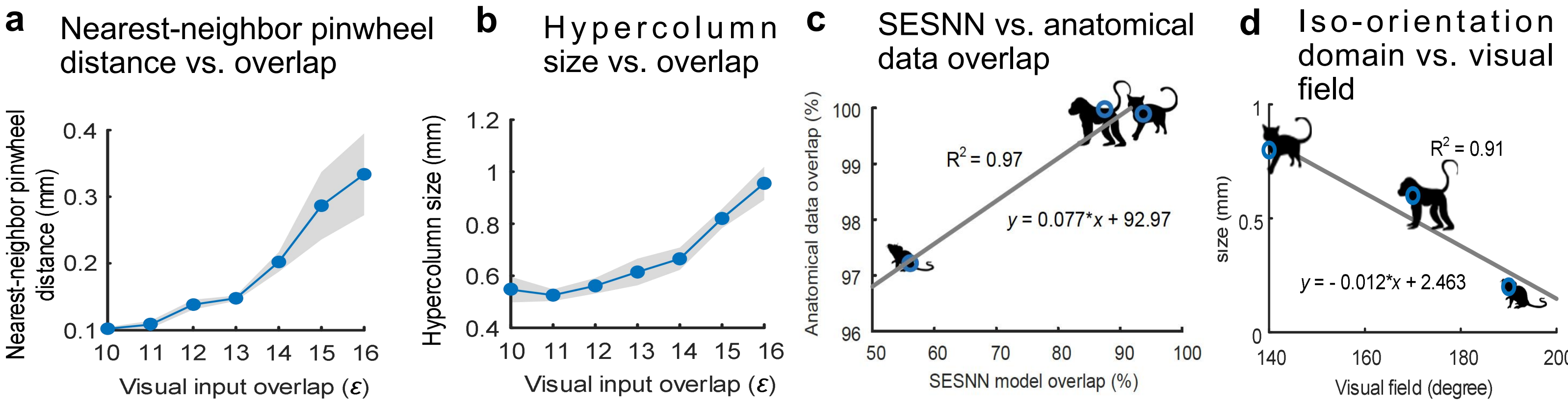

Pinwheel metrics and neuroanatomical data verification

Zhong et al. Emergent Orientation Maps —— Mechanisms, Coding Efficiency and Robustness. *ICLR 2025 spotlight.*

Role of visual field overlap in determining V1 organizations

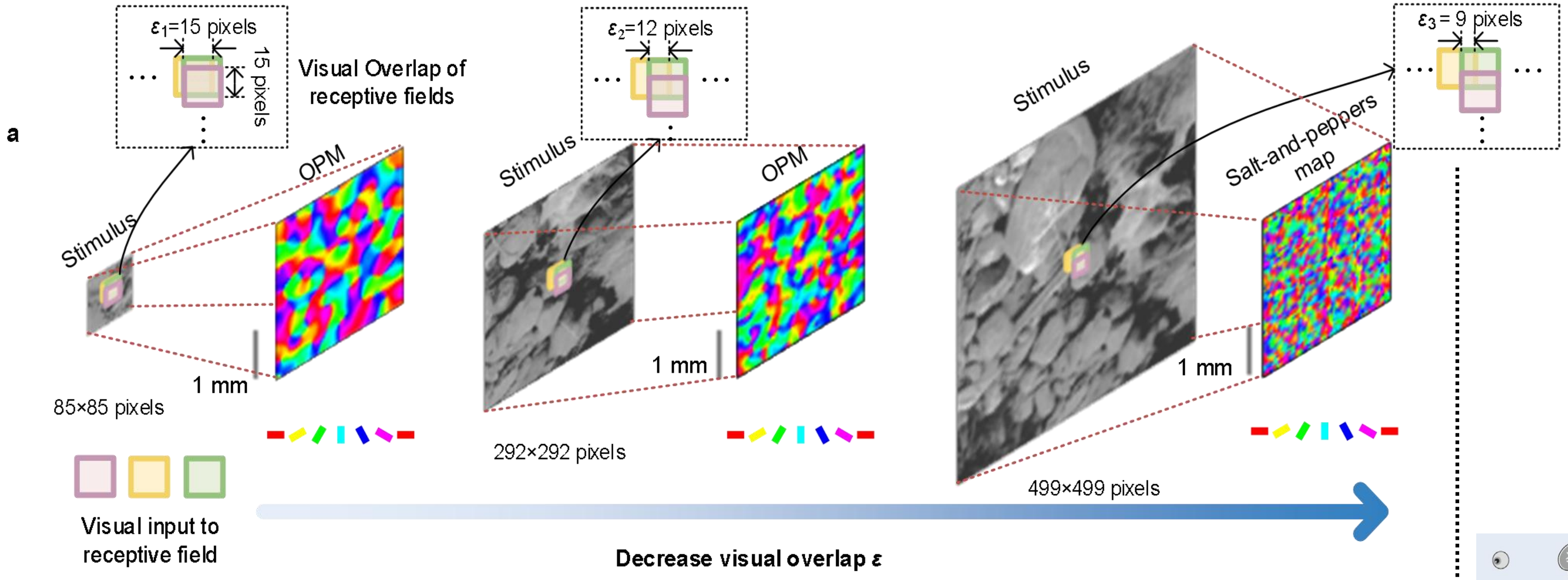

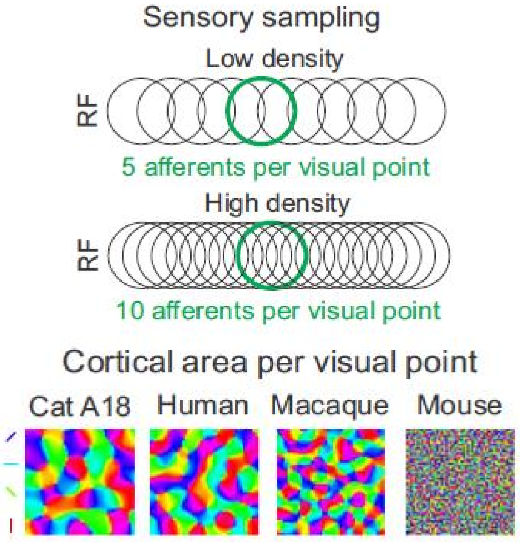

(Najafian et al., 2022, Nature Communications)

Reducing the correlation of feedforward input stimuli → plasticity adjustments (HO rule) reduce the strength of lateral synaptic connections → weaker lateral connections fail to maintain the continuity of orientation maps → resulting in a random "salt-and-pepper" orientation distribution.

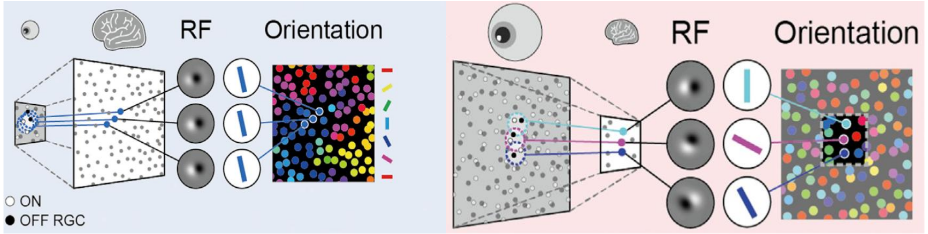

Retino-cortical mapping Ratio: $\Phi = \frac{N_{V1}}{N_{RGC}}$

(N_{V1}: number of V1 neuron, N_{RGC}: number of RGC)

High Φ value retino-cortical mapping ratio: pinwheel with **columnar structure,** Low Φ value retino-cortical mapping ratio: **salt-and-peppers.**

(Jang et al., 2020, Cell Reports)

Heterogeneous connectivity enables diverse orientation coding in pinwheels

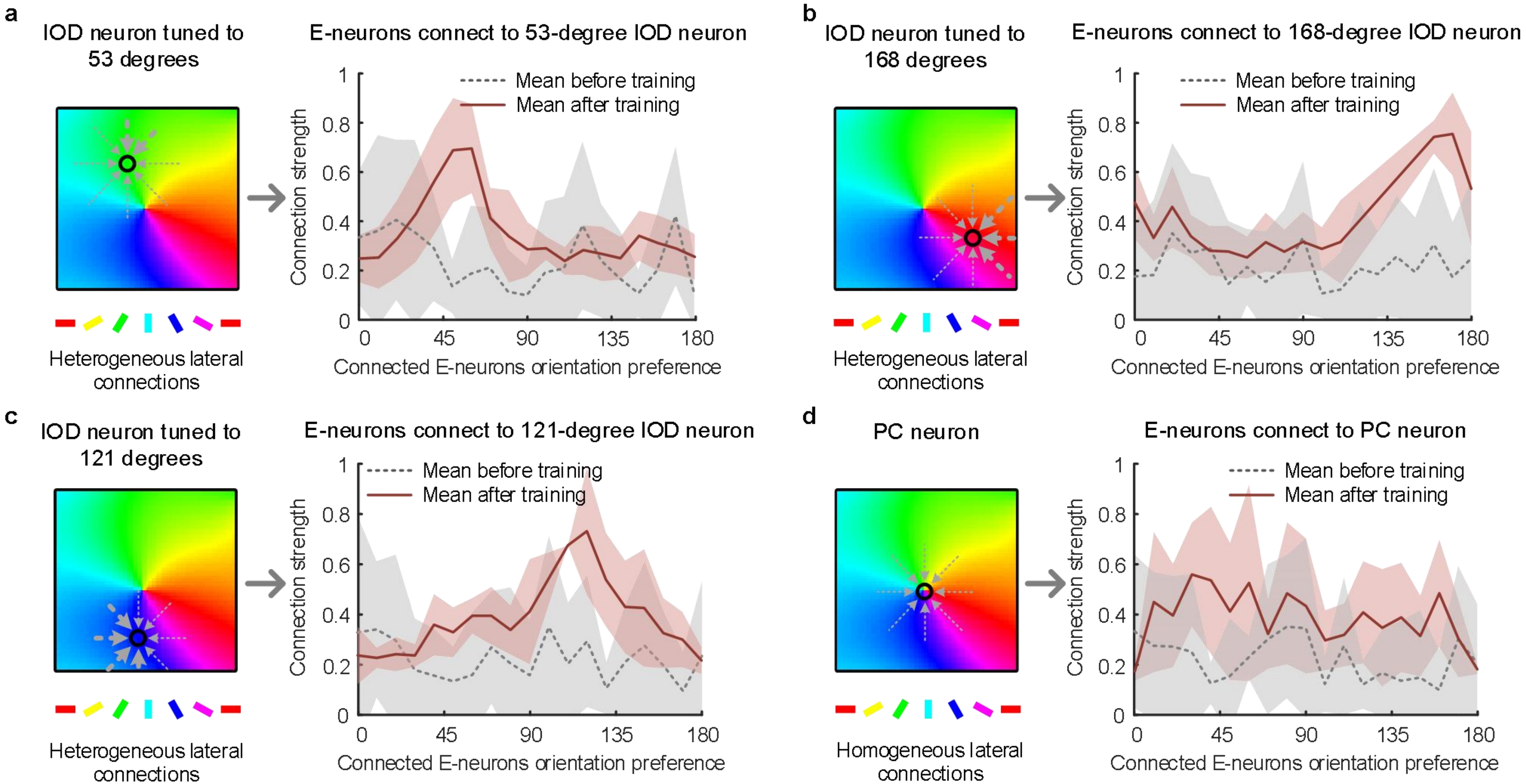

At pinwheel centers, synaptic connections from neighboring neurons exhibit relatively balanced strengths across multiple orientations, meaning these neurons receive inputs from multiple iso-orientation domains. Such balanced connectivity enables pinwheel centers to detect complex contours or intersections of multiple orientations.

Zhong et al. Emergent Orientation Maps —— Mechanisms, Coding Efficiency and Robustness. *ICLR 2025 spotlight.*

Pinwheels optimize wiring and enhance coding efficiency

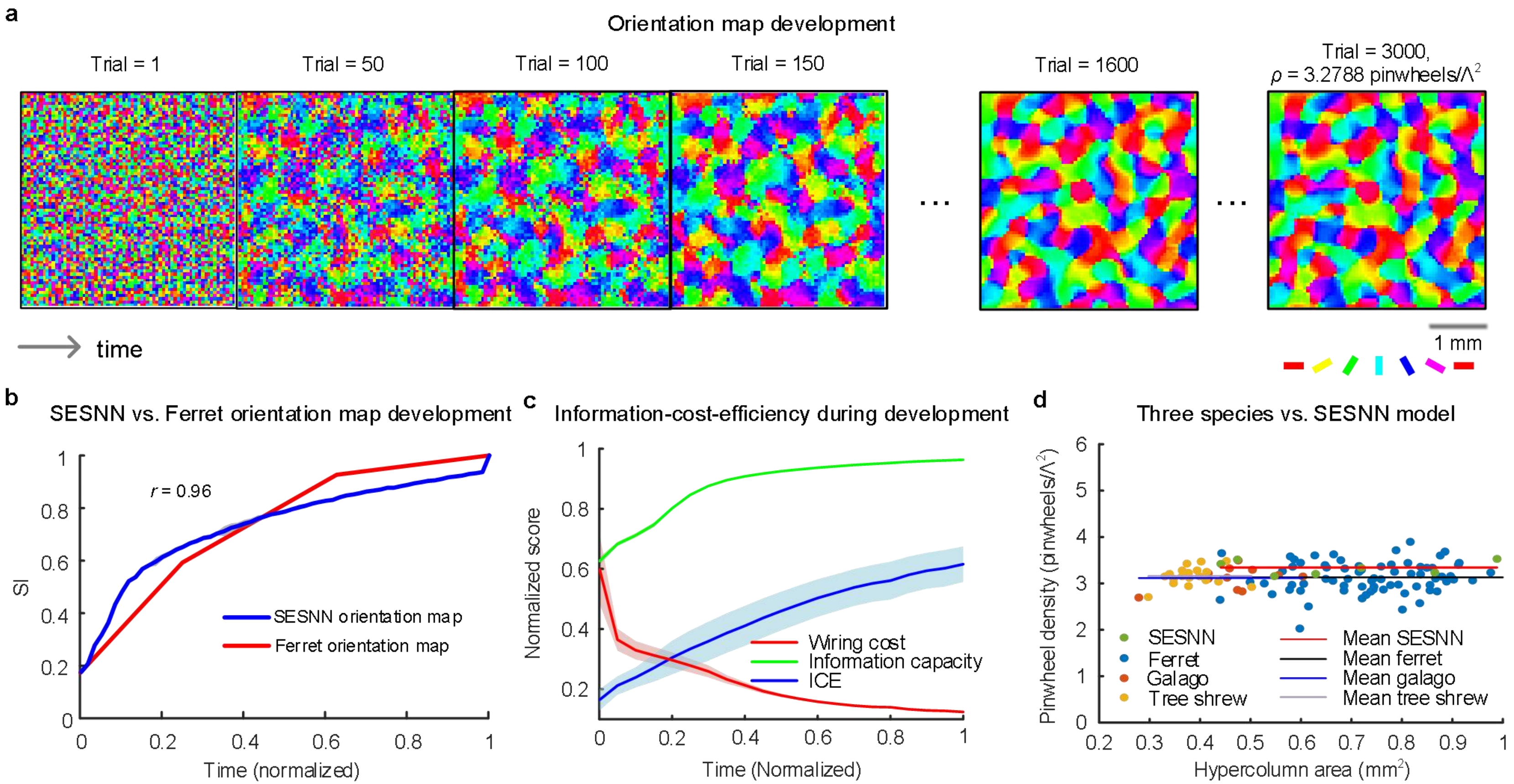

F_i = Final orientation value of pixel i. O_i = Orientation value prior developmental stage. SI (stability Index)

$$SI = 1 - \frac{4}{n\pi}\sum_{i=1}^{n}\left|(F_i - O_i)\mathrm{mod}\left(\frac{\pi}{2}\right)\right|$$

SESNN versus Ferret (Fig b).

Information-cost efficiency (ICE) that aims at measuring coding efficiency:

$$ICE = \frac{H}{C}; H = -\sum_k P_k \log(P_k); C = \sum_{i,j}\frac{1}{W_{ij}}$$

H : information encoding capacity

P_k : Discrete probability of normalized count of W_{ij} in k-bins distribution.

C : Energy cost of synaptic transmission.

- The SESNN model replicates the developmental process of pinwheel orientation maps (P33–P41), with map development closely matching experimental data.
- Beyond reducing wiring costs *(Chklovskii, 2001, Neuron)*, our results show that improved coding efficiency enables iso-orientation domains to process similar directions more effectively.

Pinwheels increase coding sparseness and robustness

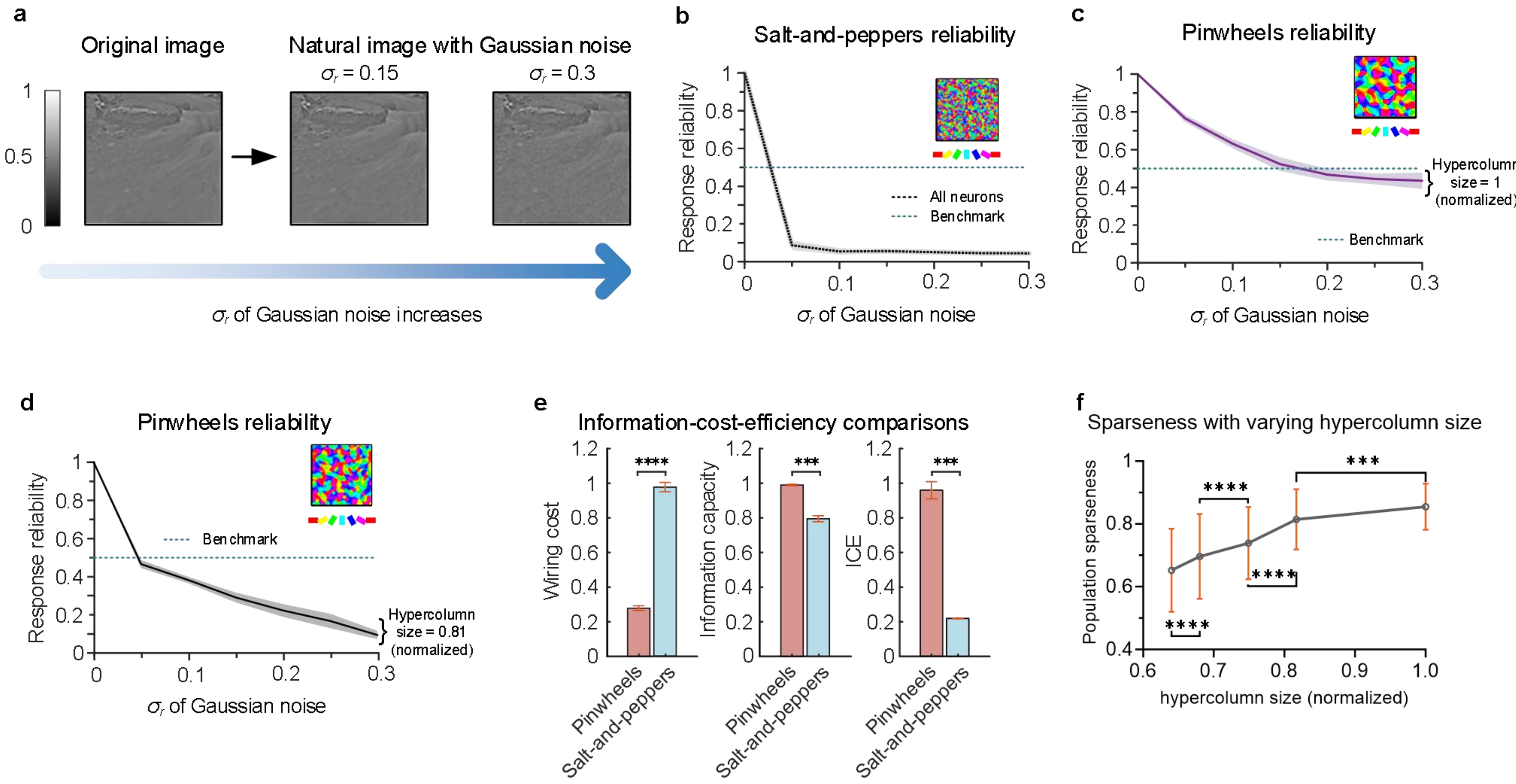

1. For each neuron, n spike trains of duration time T = 100ms are analyzed.

$$R_{xy}(m) = E[x_{T+m} y_T]$$

m: time lag, $[-\frac{T}{2}, \frac{T}{2}]$. x and y are one neuron spike train at two different trials.

2. The average $\bar{R}_{xy}$:

$$\bar{R}_{xy}(m) = \frac{\sum_{i=1}^{n} R_{xy}(m)}{n}$$

n : combinations of each two pairs within 10 trials.

3. Reliability of one neuron = $\max_{[-\frac{T}{2},\frac{T}{2}]} \bar{R}_{xy}(m)$

Population sparseness (PS):

$$PS = \frac{1-\left(\sum \frac{\langle a_i \rangle}{m}\right)^2 / \left(\sum \frac{\langle a_i \rangle^2}{m}\right)}{1-\frac{1}{m}}$$

a_i refers to the spike rate of a neuron i out of a total of m neurons in a time window.

- Compared to salt-and-peppers, pinwheel structures exhibit lower wiring costs (Fig. e), higher information-cost efficiency (Fig. e), increased sparseness (Fig. f), and greater robustness to noise (Figs. b–d), offering computational advantages.

Conclusion

- We develop a self-evolving spiking neural network based on synaptic plasticity, capable of generating both salt-and-peppers and pinwheel structures in the visual cortex.
- Mexican-hat connectivity initializes local orientation similarity and distant diversity, while visual field overlap refines E-E connections via the Hebbian-like rule, ensuring orientation continuity. E-I-E loops promote orientation diversity. Together, these factors shape distinct orientation maps.
- Neural networks with pinwheel orientation maps exhibit significantly higher coding efficiency and greater robustness to noise compared to those with salt-and-pepper maps.

ICLR
International Conference On
Learning Representations

Thank you